


# 4-Chloro-3-nitro-*N*-butylbenzenesulfonamide acts on $K_V3.1$ channels by an open-channel blocker mechanism

Carlos Alberto Zanutto Bassetto Junior<sup>1,2</sup>  · Wamberto Antonio Varanda<sup>3</sup> · Eduardo René Pérez González<sup>1,2</sup>

Received: 14 June 2017 / Accepted: 7 September 2017 / Published online: 12 September 2017  
© Springer-Verlag GmbH Austria 2017

**Abstract** The effects of 4-chloro-3-nitro-*N*-butylbenzenesulfonamide (SMD2) on  $K_V3.1$  channels, heterologous expressed in L-929 cells, were studied with the whole cell patch-clamp technique. SMD2 blocks  $K_V3.1$  in a reversible and use-dependent manner, with  $IC_{50}$  around 10  $\mu$ M, and a Hill coefficient around 2. Although the conductance vs. voltage relationship in control condition can be described by a single Boltzmann function, two terms are necessary to describe the data in the presence of SMD2. The activation and deactivation time constants are weakly voltage dependent both for control and in the presence of SMD2. SMD2 does not change the channel selectivity and tail currents show a typical crossover phenomenon. The time course of inactivation has a fast and a slow component, and SMD2 significantly decreased their values. Steady-state inactivation is best described by a Boltzmann equation with  $V_{1/2}$  (the voltage where the probability to find the channels in the inactivated state is 50%) and  $K$  (slope factor) equals to  $-22.9 \pm 1.5$  mV and  $5.3 \pm 0.9$  mV for control, and  $-30.3 \pm 1.3$  mV and  $6 \pm 0.8$  mV for SMD2, respectively. The action of SMD2 is enhanced by high frequency

stimulation, and by the time the channel stays open. Taken together, our results suggest that SMD2 blocks the open conformation of  $K_V3.1$ . From a pharmacological and therapeutic point of view, *N*-alkylsulfonamides may constitute a new class of pharmacological modulators of  $K_V3.1$ .

**Keywords**  $K_V3.1$  · *N*-alkylbenzenesulfonamides · Patch-clamp · Open-channel blockers

## Introduction

Voltage-gated potassium channels comprise a family of ion channels involved in the regulation of membrane excitability and neurotransmitter release (Hille 2001; Rodrigues et al. 2003). Abnormalities in the functioning of potassium channels may result in pathological states involving neurons, skeletal muscles, cardiac cells and epithelial cells (Shieh et al. 2000). Therefore, potassium channels are seen as therapeutic targets for an increasingly number of drugs and a multitude of studies have been conducted to unveil their functioning at molecular and systems levels.

$K_V3.1$  is a Shaw-type delayed rectifier potassium channel with very rapid activation and deactivation kinetics and a high activation threshold (Grissmer et al. 1992). These properties are crucial for high frequency firing in cells such as neurons of the medial nucleus of the trapezoid body (Wang et al. 1998; Lien and Jonas 2003; McCrossan et al. 2003), where they are responsible for imposing a rapid membrane hyperpolarization after an action potential (AP) (Yasuda et al. 2013).  $K_V3.1$  are also found in neocortical interneurons (Gan and Kaczmarek 1998; Lien and Jonas 2003), within the hippocampus (McCrossan et al. 2003), auditory system (Li et al. 2001), mouse adult neuronal stem/precursor cell (Yasuda et al. 2013) and in malignant colon cancer cells (Ousingsawat et al. 2007).

Handling Editor: E. I. Closs.

✉ Carlos Alberto Zanutto Bassetto Junior  
cbjunior@fc.unesp.br

- <sup>1</sup> Fine Organic Chemistry Laboratory, Department of Chemistry and Biochemistry, Faculty of Science and Technology, São Paulo State University (Unesp)-Campus of Presidente Prudente, Presidente Prudente, SP, Brazil
- <sup>2</sup> Post-Graduate Program in Science and Material Technology, Presidente Prudente, SP, Brazil
- <sup>3</sup> Department of Physiology, Ribeirão Preto Medical School, University of São Paulo, Ribeirão Preto, Brazil

Contrary to other families of  $K_V$  channels, the block of  $K_{V3.1}$  leads to a decrease in the AP firing frequency (Wang et al. 1998). This phenomenon is related to the activation of  $K_{V3.1}$  which starts at the falling phase of the AP. Therefore, blockade of these channels could increase the time course of the AP and slow down the firing frequency (Rudy and McBain 2001) reducing neuronal excitability. In this direction, Choi et al. (2001) suggested that fluoxetine and norfluoxetine could act as anticonvulsant drugs by blocking  $K_{V3.1}$  in a use-dependent manner. Thus, the search and development of new agents acting on  $K_{V3.1}$  channels are of both pharmacological and medical interest.

Benzenesulfonamides (amides derived from sulfanilic acid) have similarities to *p*-aminobenzoic acid (PABA), and they compete with PABA for the active site of the dihydropteroate synthase enzyme, inhibiting bacterial growth (Supuran et al. 1998). Besides this, they were reported to block  $K_{V1.5}$  channels (Gross et al. 2007, 2009; Lloyd et al. 2007; Olsson et al. 2014) and to inhibit  $K_{ATP}$  channels in beta cells of the pancreas (Hille 2001). In a previous work we reported the synthesis and chemical characterization of several benzenesulfonamide compounds (Martins et al. 2016). Here we report a detailed description of the effects of 4-chloro-3-nitro-*N*-butylbenzenesulfonamide (SMD2) on  $K_{V3.1}$  channels. We found that SMD2 acts mainly as an open channel blocker with a voltage, concentration, state and use-dependent effect.

## Experimental section

The L-929 cells stably transfected with mouse  $K_{V3.1}$  (Grissmer et al. 1994) were kindly provided to us by Dr George Chandy from the Department of Molecular Physiology at Lee Kong Chian School of Medicine, NTU (Nanyang Technological University, Singapore). L-929 cells were grown and maintained in Dulbecco's modified Eagle's Medium (DMEM) containing 10% heat-inactivated fetal bovine serum (Cultilab, Campinas, Brazil), 1 mM Na-pyruvate, 0.25 mg/ml gentamycin G-418-sulfate, 100 U/ml penicillin-G sodium and +100 µg/ml streptomycin sulfate in a humidified 5%  $CO_2$  incubator (Revco Elite II, Kendro Laboratory Products, Asheville, NC, USA) at 37 °C. Cells were detached from the culture flasks (25 cm<sup>2</sup>) with trypsin/EDTA solution, seeded on glass coverslips, maintained in DMEM and used within 2–8 h for electrophysiological experiments.

Electrophysiological recordings were performed according to Hamill et al. (1981) and Rodrigues et al. (2003). The bath solution contained (in mM) 155 NaCl, 1 MgCl<sub>2</sub>, 2 CaCl<sub>2</sub>, 5 HEPES and 4.5 KCl, pH 7.4 (NaOH) and osmolality 300–310 mosm/Kg H<sub>2</sub>O. The pipette solution had the following composition (in mM) 140 KF, 5 EGTA, 10 HEPES, 2 MgCl<sub>2</sub> and 1 CaCl<sub>2</sub>, pH 7.2 (KOH)

and osmolality 290–300 mosm/Kg H<sub>2</sub>O. Borosilicate glass micropipettes (BF-150-86-15, Sutter Instrument, Novato, CA, USA) were pulled in a horizontal puller (SP-97, Sutter Instrument), and had resistance ranging from 2 to 4 MΩ when backfilled with the pipette solution. Series resistance ranged from 4 to 10 MΩ and was electronically compensated up to 80% when the current exceeded 2 nA. The junction potential between the bath and pipette solutions was calculated using Clampex (Molecular Devices, Sunnyvale CA, USA) and experimentally measured, resulting in –8.4 and –8 mV, respectively, and corrected offline. All experiments were performed at room temperature (23 °C).

Ionic currents in response to voltage steps were measured with an Axopatch 200B (Molecular Devices). Currents were low-pass filtered at 5 kHz and fed to a computer through an A/D D/A converter (ITC-16 Computer Interface—Instrutech Corp., Great neck, NY, USA). The software WinWCP (Strathclyde Electrophysiology Software, ©John Dempster, University of Strathclyde, Glasgow, Scotland), was used for data acquisition and pulse generation. Cells were maintained at a holding potential of –88 mV in all cases and they were superfused during the whole experiment with control solution, or with solution containing a given drug concentration using a rapid solution changer (RSC-160, Bio-logic Science Instruments SAS, Calix, France). The voltage pulse protocols and sampling frequency will be described under the particular result. The procedures used for synthesis and chemical characterization of 4-chloro-3-nitro-*N*-butylbenzenesulfonamide can be found in Martins et al. (2016), where it was called compound 3, and references therein.

Before use, SMD2 was first dissolved in 0.5 M NaOH resulting in a 10 mM stock solution and then diluted in bath solution to the desired concentration. The osmolality of the final solutions containing SMD2 was in the range 306–313 mosm/Kg H<sub>2</sub>O, and it was not significantly different from the osmolality of the bath solution. The pH was adjusted to 7.4 with HCl. The amount of Na<sup>+</sup> added to the solution containing 13.5 µM SMD2 changed the final sodium concentration by only 0.675 mM and was not taken into consideration.

The total charge transferred was calculated in each case by integrating the current trace for the duration of the applied voltage pulse. The fractional remaining current ( $\frac{I}{I_{CTRL}}$ ) or fractional remaining charge transferred ( $\frac{Q}{Q_{max}}$ ) was plotted against the concentration of the drug. The Hill equation for current,  $\frac{I}{I_{CTRL}} = \frac{IC_{50}^N}{IC_{50}^N + (D)^N}$ , and for charge  $\frac{Q}{Q_{CTRL}} = \frac{IC_{50}^N}{IC_{50}^N + (D)^N}$ , was fitted to the data points. Here, *D* is the concentration of SMD2,  $IC_{50}$  is the concentration where the remaining current or charge is equal to 50% of the control, and *N* is the Hill coefficient.

Where pertinent, a standard form of the Boltzmann equation, as shown below, was adjusted to the data points:

$$y = 1/[1 + \exp((V - V_{1/2})/K)],$$

where  $V_{1/2}$  is the voltage at which 50% of the channels are in a determined state,  $V$  is the voltage across the membrane and  $K$  is a slope factor. In the presence of SMD2, the sum of two Boltzmann functions was required for a good fit:

$$y = 1/[1 + \exp((V - V_{1/2}^1)/K^1)] + 1/[1 + \exp((V - V_{1/2}^2)/K^2)],$$

where  $V_{1/2}^1$  and  $V_{1/2}^2$  are the voltages where 25 and 75% of the channels are open, respectively.  $K^1$  and  $K^2$  are the slope factors for the first and second processes, respectively.

The time courses of the tail currents were fitted with the sum of exponential functions, of the type  $y = y_0 + A_n \exp(t/\tau_n)$ . The number of terms used will depend on the particular kind of experiment. Data analysis was done with the software Origin 8.0 (Origin Lab Corp., Northampton, MA, USA) and Clampfit (PCLamp 10, Molecular Devices).

Data are presented as the mean  $\pm$  SEM. Student's paired  $t$  test was used for statistical comparison of data sets and  $P < 0.05$  indicates a statistically significant difference. All chemical compounds were purchased from Sigma (Sigma-Aldrich®, St Louis, MO, USA).

## Results

The basic effects of SMD2 on K<sub>v</sub>3.1 channels are shown in Fig. 1. In accordance with previous results, Fig. 1a shows that K<sub>v</sub>3.1 currents activate rapidly and inactivate slowly (Grissmer et al. 1992; Aiyar et al. 1994; Sung et al. 2008; Taskin et al. 2015). SMD2 affects both the amplitude of the K<sub>v</sub>3.1 currents at the end of the pulse and the kinetics of the descending phase with a minor effect on the peak of the currents (Fig. 1b). Figure 1c shows the mean values of currents against voltage in control and in the presence of SMD2. The effect is larger when measured at the end of the pulse ( $37.9 \pm 0.9\%$  of the current remains at +92 mV; square symbols) than at the peak ( $89.2 \pm 3.1\%$  of the current remains at +92 mV; circles). Therefore, to better characterize the effects, we also choose to measure the total charge transferred during the voltage pulse, since this parameter would take into consideration the effect on the amplitudes and on the kinetics of the currents. These data are shown in Fig. 1d. SMD2 has an intense effect on the total charge transferred by K<sub>v</sub>3.1 channels, blocking

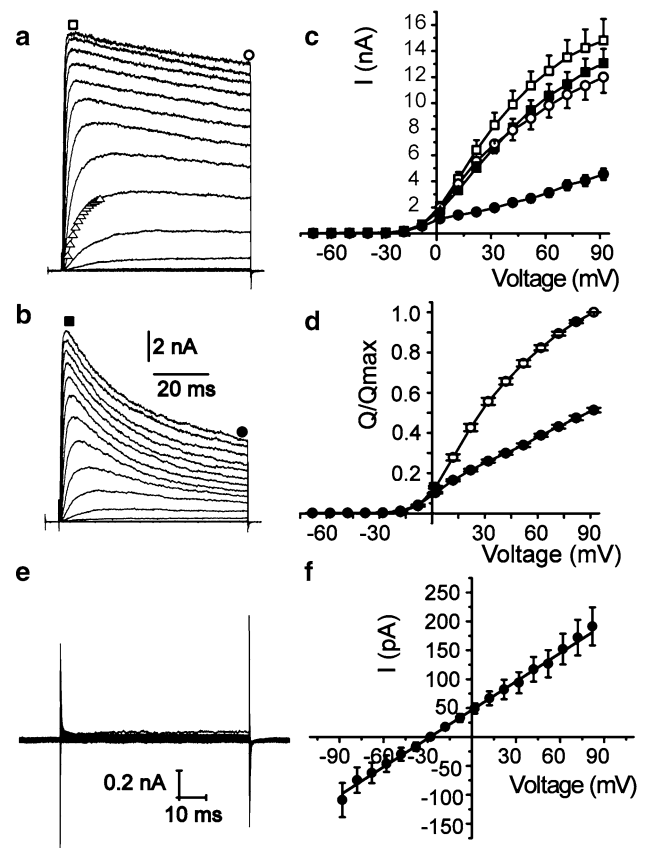


**Fig. 1** SMD2 blocks K<sub>v</sub>3.1 channels. **a, b** Current traces from cells held at  $-88$  mV and pulsed to  $+92$  mV, in  $10$  mV steps for  $70$  ms in control and in the presence of  $13.5$   $\mu$ M SMD2, respectively. Open triangles superimposed on the traces are exponential fits to the data points used to analyze the kinetics of the process, as shown in Fig. 5. Squares and circles on top of traces in **a** and **b** show the points where the currents were measured (peak; open squares = control, filled squares =  $13.5$   $\mu$ M SMD2) (end of the pulse; open circles = control, filled circles =  $13.5$   $\mu$ M SMD2), respectively). **c**  $I$  vs  $V$  relationship for the peak and for the end of the voltage pulse ( $n = 5$ ). **d** Relationship between the normalized total charge transferred ( $Q/Q_{\max}$ ) and voltage for control (open circles) and in the presence of  $13.5$   $\mu$ M SMD2 (filled circles). Normalization was done by dividing each value of total charge by its value at  $+92$  mV, observed in the control condition ( $N = 5$ ). **e** Shows representative traces of currents measured in wild type L-929 cells. The currents were elicited from a holding potential of  $-88$  mV and pulsed to  $+82$  mV, in  $10$  mV steps for  $70$  ms. **f** Current versus voltage relationship for the currents shown in **e**. The solid line is a linear fit to the experimental points. The reversal potential is about  $-30$  mV for L-929WT. The data are shown as Mean  $\pm$  SEM ( $N = 9$ )

$54.0 \pm 2.1\%$  at  $+32$  mV and  $50.1 \pm 1.7\%$  at  $+92$  mV. Figure 1e, f, shows results from measurements performed on wild type (non-transfected) L-929 cells. As can be seen, the currents present very small amplitudes and the responses are linear, not displaying significant rectification. These results assure us that the currents measured

in transfected L-929 cells are being carried by  $K_{V3.1}$  channels.

### Dose–response relationship

Figure 2a shows typical current traces in response to voltage pulses from  $-88$  to  $+32$  mV, (duration = 70 ms; holding potential =  $-88$  mV) for several concentrations of SMD2. As the concentration increases, the magnitude of the peak current and the current at the end of the pulse decrease and with a faster decay time course. Nevertheless, a small initial peak is still observed even for the highest concentration used. Figure 2b shows dose–response relationships using the amplitude of the currents at 70 ms and the total charge transferred during the pulse, for concentrations of ( $\mu\text{M}$ ) 1, 3, 5, 10, 20, 40, 60 and 80. Fits of the Hill equation to the data points resulted in  $IC_{50}$  equal to  $9.3 \pm 0.6 \mu\text{M}$  for the current and  $13.5 \pm 0.5 \mu\text{M}$  for the charge. The Hill coefficients are  $1.9 \pm 0.1$  for current and  $1.7 \pm 0.1$  for charge, respectively. The difference in the values of  $IC_{50}$  obtained in each condition is one of the several indicators that SMD2 acts as open-channel blocker. Additionally, the binding of  $100 \mu\text{M}$  of SMD2 to the channel is readily reversible, since washing out of the drug brings the currents to value corresponding to at least 87% of the control values, as demonstrated by data in Fig. 2c.

### The voltage dependence of block

Figure 3a shows that channels start to open at voltages around  $-20$  mV and the conductance rises steeply with depolarizations up to  $+32$  mV. The effect of SMD2 ( $13.5 \mu\text{M}$ ) is shown by the filled circles, as fraction of block ( $F_{\text{block}}$ ) measured at the end of the voltage pulse. It is clearly seen that  $F_{\text{block}}$  reaches almost 70% at  $+32$  mV and then starts to decline for depolarizations larger than this value. The coincidence of stronger block in a voltage range when channels are opening is consistent with the hypothesis that SMD2 acts as an open channel blocker. Besides this, it should be noticed that there is a relief of block at larger depolarizations. In agreement with the results shown in Fig. 3a, the relationship between  $G_{\text{norm}}$  and voltage can be accurately described by a single Boltzmann function in the control situation, as shown in Fig. 3b (open circles).  $V_{1/2}$  and  $K$  (slope factor) are  $14.2 \pm 1.1$  and  $10.1 \pm 0.6$  mV, respectively, as expected for  $K_{V3.1}$  channels and reported by others (Grissmer et al. 1992). On the other side, in the presence of SMD2 (filled circles) the relationship between  $G_{\text{norm}}$  and voltage requires the sum of two Boltzmann functions, to be properly described. The curve is strongly shifted to the left and the voltage dependence is shallower than the control. This may reflect the

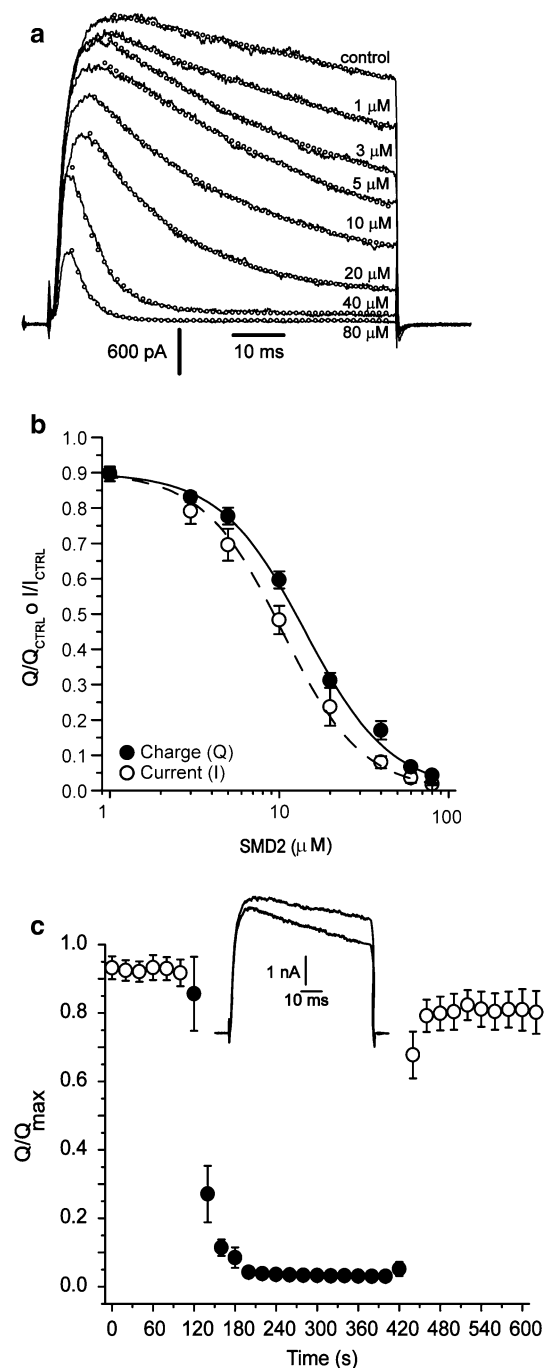


**Fig. 2** Basic blocking properties of SMD2 at  $K_{V3.1}$ . **a** Representative traces of currents elicited by a depolarizing voltage pulse from  $-88$  to  $+32$  mV, for 70 ms, in control and in the presence of several SMD2 concentrations, as indicated. **b** Normalized current ( $I/I_{\text{max}}$ ) or charge transferred ( $Q/Q_{\text{max}}$ ) versus concentration of SMD2, for each condition. The continuous line is a best fit of the Hill equation to the data points ( $n = 9$  cells). **c** The effect of  $100 \mu\text{M}$  of SMD2 (filled circles) is reversible upon washout. The inset illustrates representative current traces in each condition, elicited by a depolarization to  $+32$  mV from a holding of  $-88$  mV. Upper tracer = control; middle trace = after washout and lower gray trace = in the presence of SMD2 ( $N = 5$ )

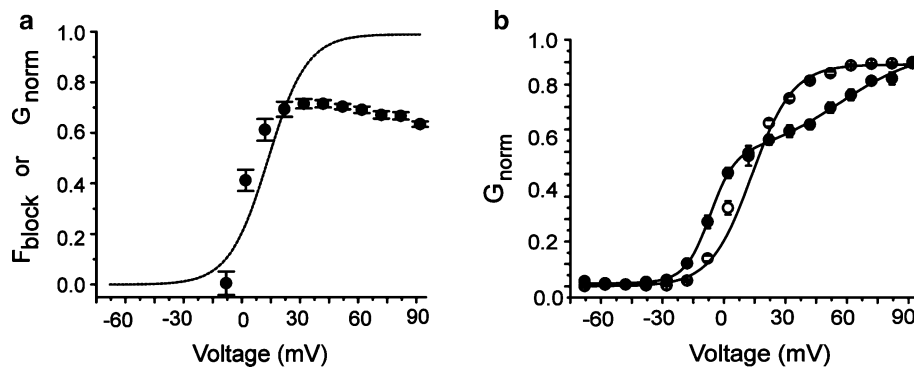


**Fig. 3** Block by SMD2 is voltage dependent. **a** Fractional block ( $F_{\text{block}} = 1 - I_{\text{SMD2}}/I_{\text{CTRL}}$ ) of  $K_v3.1$  channels for  $13.5 \mu\text{M}$  SMD2 (filled circles). The continuous line is the activation curve for the channel expressed as  $G_{\text{norm}} \times V$  and taken from **b**. The effect of SMD2 is strongly voltage dependent in the range from approximately  $-10$  mV up to  $+32$  mV, where channels are being opened by voltage ( $n = 8$ ). **b** Normalized conductances (current measured at the end of the pulse) for control (open circles) and in the presence of SMD2 (filled

circles). A standard Boltzmann function is sufficient to describe the experimental data in the control situation. The values for  $V_{1/2}$  and  $K$  are equal to  $14.2 \pm 1.1$  mV and  $10.1 \pm 0.6$  mV, respectively. In presence of SMD2, the sum of two Boltzmann functions are necessary to accurately describe the data. The derived parameter values are  $V_{1/2}^1 = -6.9 \pm 0.7$  mV,  $K^1 = 6.0 \pm 0.8$  mV,  $V_{1/2}^2 = 56.3 \pm 4$  mV and  $K^2 = 20.3 \pm 6.6$  mV ( $N = 8$ )

block relief, at high depolarizations, and is in accordance with data in Fig. 3a.

### SMD2 does not alter the selectivity of $K_v3.1$

For measuring the selectivity of the  $K_v3.1$  channels, we evaluated the charge transferred in tail current experiments, as described in Fig. 4. Tail currents have their time scale expanded to better appreciate the time course of the events as show in the representative traces in Fig. 4a (control) and b (in the presence of  $13.5 \mu\text{M}$  SMD2). Figure 4c shows the

charge transferred as a function of the applied voltage. The intercept of the curves describing the data points with the voltage axis gives us the reversal potential, which is practically the same for control and in the presence of SMD2.

### Effects of SMD2 on the activation and deactivation kinetics of $K_v3.1$

$K_v3.1$  are fast activating channels with the current rising to a peak within a few milliseconds. Time constants of activation ( $\tau_{\text{activation}}$ ) were calculated by adjusting a single exponential

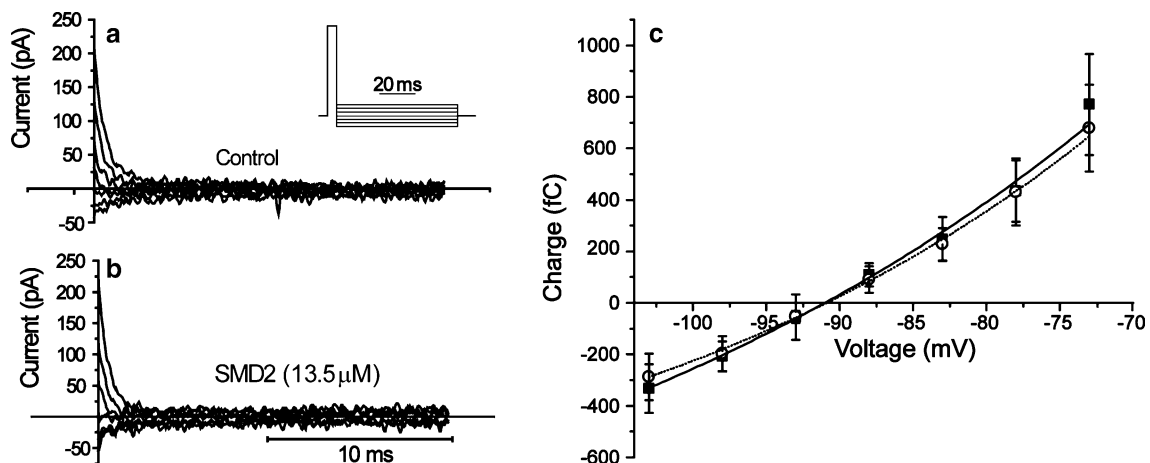


**Fig. 4** SMD2 does not alter the selectivity of the  $K_v3.1$  channels. **a** Tail currents elicited in response to voltage pulses in control and **b** in presence of SMD2. Tail currents were elicited by 70 ms hyperpolarizing voltage pulses from  $-103$  to  $-73$  mV, in 5 mV steps, after a depolarization from  $-88$  to  $+32$  mV for 5 ms, applied every 20 s (inset). For each trace, the charge transferred for control (open circles) and

in the presence of SMD2 (filled circles), was calculated and plotted against voltage in **c** ( $N = 9$ ). Note that the reversal potential is around  $90.9 \pm 1$  mV in the absence and  $-91.1 \pm 1.3$  mV in presence of the drug. The theoretical reversal potential expected from the Nernst equation is equal to  $-90.1$  mV

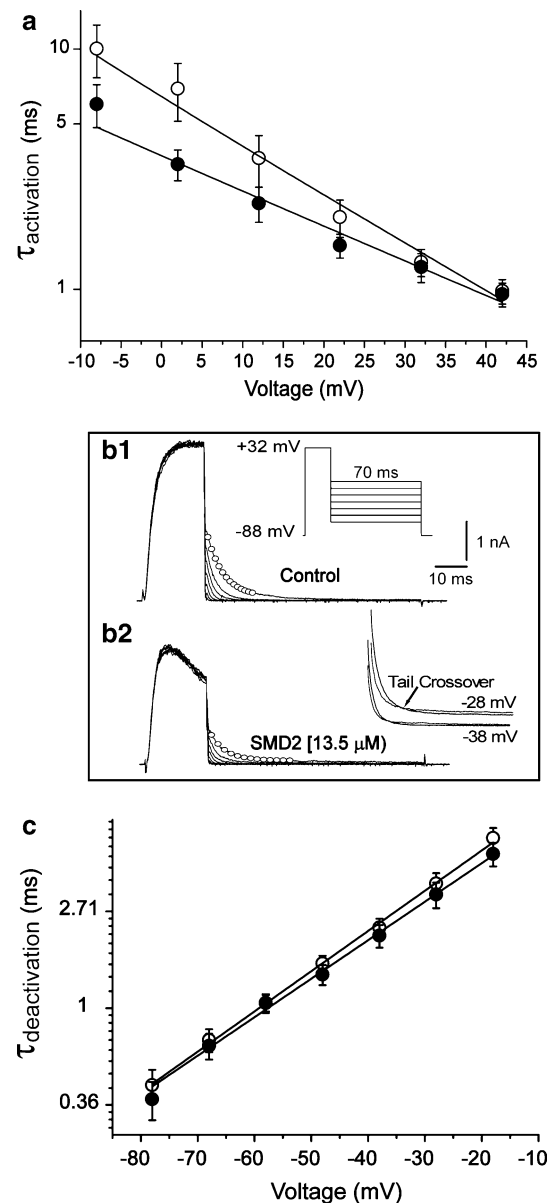


**Fig. 5** SMD2 affects the opening and closing rates of  $K_v3.1$  channels. **a** Time constant of activation ( $\tau_{\text{activation}}$ ) were calculated by adjusting a single exponential function between 10 and 90% of the rising phase of the current traces, as shown in Fig. 1a, and plotted against voltage. For depolarizations up to +42 mV, the relationship is best described by a single exponential function, varying e-fold every  $21.3 \pm 1.4$  mV in control (open circles) and e-fold every  $29.3 \pm 2.6$  mV in presence of SMD2 (solid circles) ( $n = 6$ ). **b1** Representative traces of tail currents used to estimate the time constant of deactivation of the channels ( $\tau_{\text{deactivation}}$ ) in control and **b2** in the presence of  $13.5 \mu\text{M}$  SMD2. Channels were first activated by a voltage pulse to +32 mV (holding = -88 mV) for 20 ms, and then closed by hyperpolarizing the voltage between -78 and -28 mV, in 10 mV steps, for 70 ms.  $\tau_{\text{deactivation}}$  was calculated by fitting a single exponential function between 10 and 90% of the decay phase of the tail currents. The inset shows the closing kinetics in an expanded time scale to better visualize the crossing over of currents induced by SMD2 gray lines represents tail currents in presence of  $13.5 \mu\text{M}$  SMD2 and black lines represents tail currents in control situation. **c**  $\tau_{\text{deactivation}}$  against voltage varies e-fold every  $24.4 \pm 1.1$  mV in control (open circles) and e-fold every  $25.6 \pm 1.1$  mV in the presence of SMD2 (solid circles) ( $N = 11$ )

function to the rising phase of the current traces as shown in Fig. 1a (open triangles) and the results plotted against voltage in Fig. 5a. Although  $\tau_{\text{activation}}$  is poorly voltage dependent, SMD2 induces a faster activation for voltages less depolarized than around +42 mV and shallower voltage dependence. Deactivation was analyzed by measurements of the decay phase of tail currents, shown as open circles in Fig. 5b. The voltage dependence is not critically affected by SMD2, but the tail currents show crossover (inset to Fig. 5b1), a typical effect that reinforces the suggestion of an open channel blocker mechanism. SMD2 has only a minor effect on the voltage dependence of deactivation (Fig. 5c), not significantly different from control. This may indicate that closure is achieved only after the unbinding of SMD2 from the channel.

### Current decay after channel opening

The effects of SMD2 on steady-state inactivation are shown in Fig. 6. The fraction of current remaining in response to long voltage pulses (Fig. 6a) is plotted against voltage in Fig. 6b. SMD2 shifts the inactivation curve to the left ( $\sim 8$  mV—Fig. 6b), indicating that less depolarization is needed to get the same degree of inactivation. Although  $V_{1/2}^{\text{inac}}$  in control and in the presence of SMD2 were significantly different, the voltage dependence of the system is practically the same for both conditions  $K_{\text{inac}}$  is 5.3 mV in control and 6.0 in the presence of SMD2 (not significantly different). This is in accordance with the idea that SMD2 needs to unbind before the channel could enter the inactivated state.  $K_v3.1$  channels inactivate slowly, requiring voltage pulses longer than 1 s to observe full inactivation. This can be seen in Fig. 6c where a depolarization to +32 mV was applied for



5 s. Two points are clear from these results; (1) the inactivation process is best described by the sum of two exponential functions with a fast and a slow component and (2) SMD2 makes the decaying phase of the current faster, by affecting both time constants (Fig. 6d). SMD2 causes a 68% reduction in the fast component and only 47% in the slow component. This indicates that SMD2 affects mostly the open channel with minor effects on the inactivation per se.

### Recovery from inactivation

A classical double depolarizing voltage pulse protocol was applied to the cells to analyze recovery from inactivation. The duration of the pulses was kept constant at 200 ms and the interpulse interval was varied as shown in Fig. 7a. For

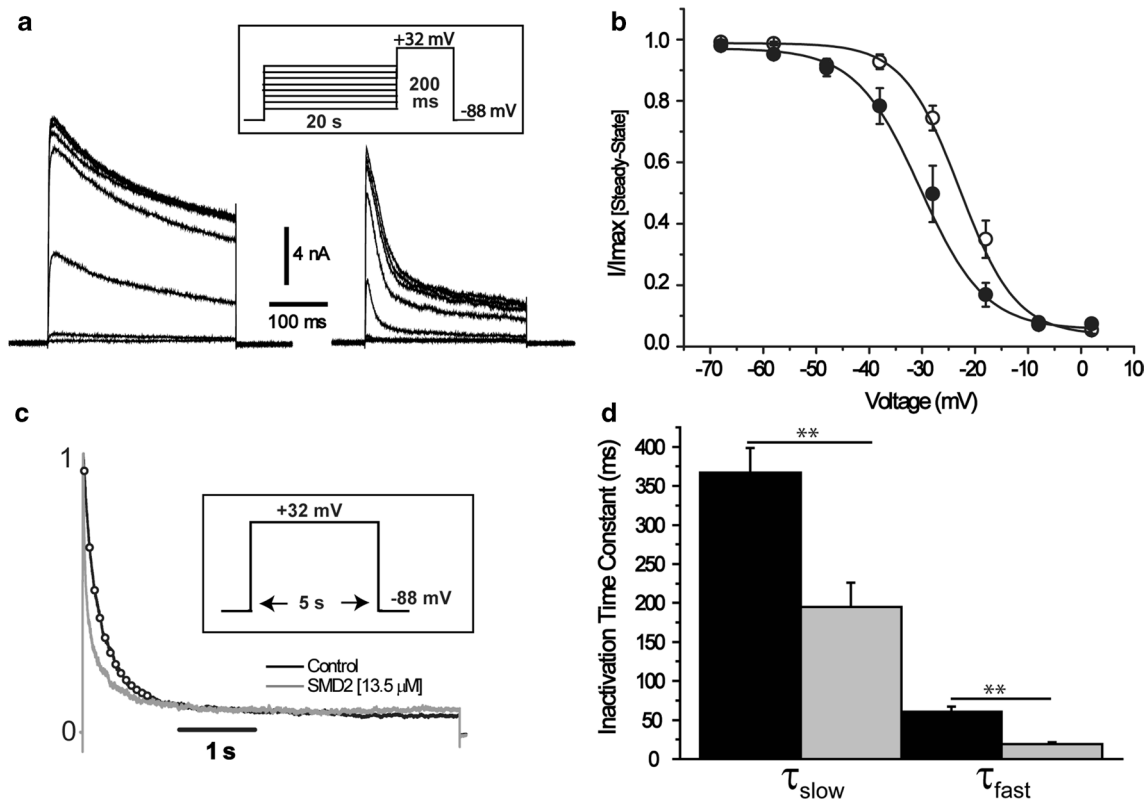


**Fig. 6** SMD2 shifts the inactivation curve to the left. **a** Representative traces showing the time course of the inactivation (right = control; left = in the presence of SMD2). The steady-state inactivation was measured by applying conditioning voltage pulses ranging from  $-88$  to  $+2$  mV, for 20 s, before the test pulse to  $+32$  mV, for 300 ms, in control and presence of  $13.5 \mu\text{M}$  SMD2. The pulse protocol is shown in the inset. **b** Normalized steady-state currents versus the conditioning voltages. Data points are described by a Boltzmann equation with  $V_{1/2}^{\text{inac}}$  and  $K$  equal to  $-22.9 \pm 1.5$  mV and  $5.3 \pm 0.9$  mV for control and  $30.3 \pm 1.3$  mV and  $6 \pm 0.8$  mV for SMD2, respectively.  $V_{1/2}^{\text{inac}}$  values are significantly different, while the  $K_{\text{inac}}$  are not

( $n = 6$ ). **c** Inactivation time course was measured after a depolarizing voltage pulse from  $-88$  to  $+32$  mV, for 5 s. A double exponential function was adjusted to the data points (open circles) and the respective time constants calculated.  $\tau_{\text{slowCTRL}} = 367 \pm 31.7$  ms and  $\tau_{\text{fastCTRL}} = 60.7 \pm 6.5$  ms. SMD2 decreased these values to  $195.1 \pm 30.8$  ms and  $19.5 \pm 2$  ms, respectively. Traces shown were normalized in relation to the peak to emphasize the time course information ( $N = 8$ ). **d** Bar graph of the time constants in control and in the presence of SMD2. Asterisks indicate statistically significant differences

short pulse intervals, the second peak of current is decreased in relation to the first, both for control and in presence of SMD2. As the interpulse interval is increased, the ratio of the second by the first peak of current are increased, indicating that recovery is slowed when the channel is blocked (Fig. 7b, c). The time for recovery of the current is quantified in Fig. 7d. The recovery time constants,  $\tau_1$  and  $\tau_2$ , are  $1.0 \pm 0.4$  s and  $0.03 \pm 0.05$  s for control and  $1.2 \pm 1$  s and  $0.06 \pm 0.04$  s for SMD2, respectively. The values of  $\tau_1$  and  $\tau_2$  in control conditions were significantly different when compared with  $\tau_1$  and  $\tau_2$  in the presence of SMD2. Therefore, SMD2 slows down the recovery rates of  $K_V3.1$ , once again indicating that SMD2 must leave the channel for inactivation to take place.

### Use-dependent effects of SMD2

Since SMD2 binds to the open conformation of the  $K_V3.1$  channels, we tested if the time that the channel stays open influences the effect of SMD2. A voltage protocol in which the depolarization time (from 2 to 20 ms) is varied between pulses, with a fixed interpulse interval (20 ms), was applied to the cells. In Fig. 8b–d, the representative traces of the current responses are shown. The longer the pulse duration, the stronger is the blocking effect of SMD2. This observation is better visualized in Fig. 8e, where the effect of SMD2 on the ratio of the amplitudes of a given peak and the first peak decreases as the number of pulses and the duration of each one is increased. For example, for pulse duration of 2 ms, the per cent decay of the peak ratio is negligible, while in the presence of SMD2 the ration decreases to about 80% of the control at the last pulse (circles). For pulse duration

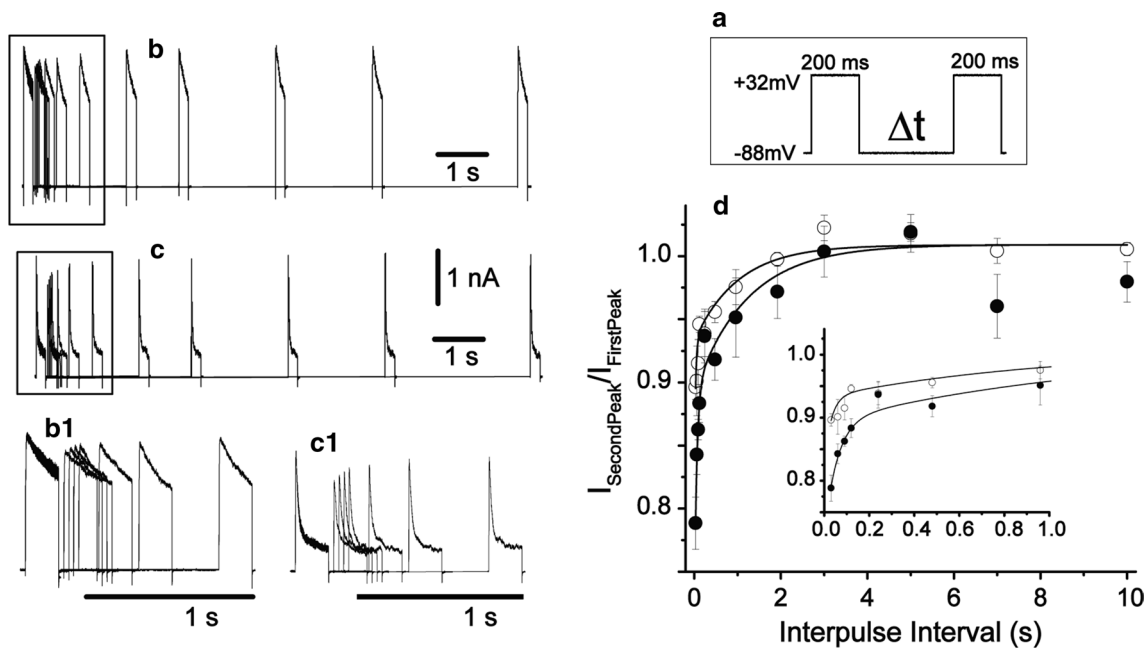


**Fig. 7** SMD2 changes the rate of recovery from inactivation of  $K_{v3.1}$  channels. **a** Voltage protocol depolarizing pulses were applied from  $-88$  mV to  $+32$  mV, for 200 ms, and the interval between successive pulses was increased in the following order 0.030, 0.060, 0.120, 0.240, 0.480, 0.960, 1.920, 3, 5, 7 and 10 s. **b** Representative sequence of current responses to the pulses, in control, and **c** in presence of  $13.5$   $\mu$ M SMD2. To better visualize the effect of SMD2 upon recovery, **b1** and **c1** show expanded versions of the region inside the rectangles ( $\Delta t < 1920$  ms) in **b** and **c**, respectively. **d** Plot of the nor-

malized second peak amplitude in relation to the amplitude of the first peak, against the interpulse interval. Inset is a zoom in the region of interpulse intervals less than 1 s. Open circles are data in control and filled circles in the presence of SMD2. Solid lines are best fits of double exponential functions to the data points in each situation. The time constants,  $\tau_1$  and  $\tau_2$ , were  $1.0 \pm 0.4$  s and  $0.03 \pm 0.05$  s for control and  $1.2 \pm 1$  and  $0.06 \pm 0.04$  in the presence of SMD2, respectively. Both  $\tau_1$  and  $\tau_2$  were significantly different ( $N = 6$ )

of 20 ms (lozenges), the last response decreases to 63% of the first peak value in control and to 40% in the presence of SMD2. What really changes is the time to reach an apparent steady state. This is reinforced by the data in Fig. 8f, where  $\tau$  decreases with pulse duration. This result also suggests that SMD2 acts mainly in the open state and not on the inactivated state of the channel. Another point of interest is that even with a depolarization as short as 2 ms, there is time for binding of the drug to the  $K_{v3.1}$  channel.

### Closing rates under high frequencies of stimulation

The blocking effect of SMD2 as a function of the opening frequency of  $K_{v3.1}$  channels was analyzed in the following set of experiments. Short depolarizing voltage pulses (5 ms duration) with a variable time between the first and the subsequent pulses were applied to the cells resulting in the following frequencies of stimulation 10, 12.5, 22.2, 40, 100, 125, 142, and 166.7 Hz. Figure 9b–d show the current responses for the frequencies of 22.2, 100 and 166.7 Hz, respectively. The responses to the subsequent pulses become smaller as the frequency increases, indicating that the more frequently the channels open, the higher is the chance to be

blocked. Additionally, for frequencies higher than 66 Hz, the relationship between  $I_{\text{Peak}}/I_{\text{FirstPeak}}$  against time (Fig. 9e), in the presence of SMD2, requires two exponential functions to be properly described. More interesting is that the time constants of the slow components have about the same value for both control and in the presence of SMD2, in the range 200–700 ms (Fig. 9f). The fast component (Fig. 9g) has values ranging from 33 (66.7 Hz) to 24 (166.7 Hz) ms. Both parameters varied almost linearly with frequency. The fact that the slow time constants have similar values in control and with SMD2 may indicate that they are describing mostly the closing of the channels. And the appearance of a fast component in presence of SMD2, at higher frequencies, is certainly associated with the open block mechanism.

### Discussion

Benzenesulfonamides are mainly known for their effects as antibacterial agents. In this study, we tested the hypothesis that 4-chloro-3-nitro-*N*-butylbenzenesulfonamide (SMD2) acts on  $K_{v3.1}$  channel, a member of the voltage dependent potassium channel family  $K_{v3}$  (Grissmer et al. 1992). Here



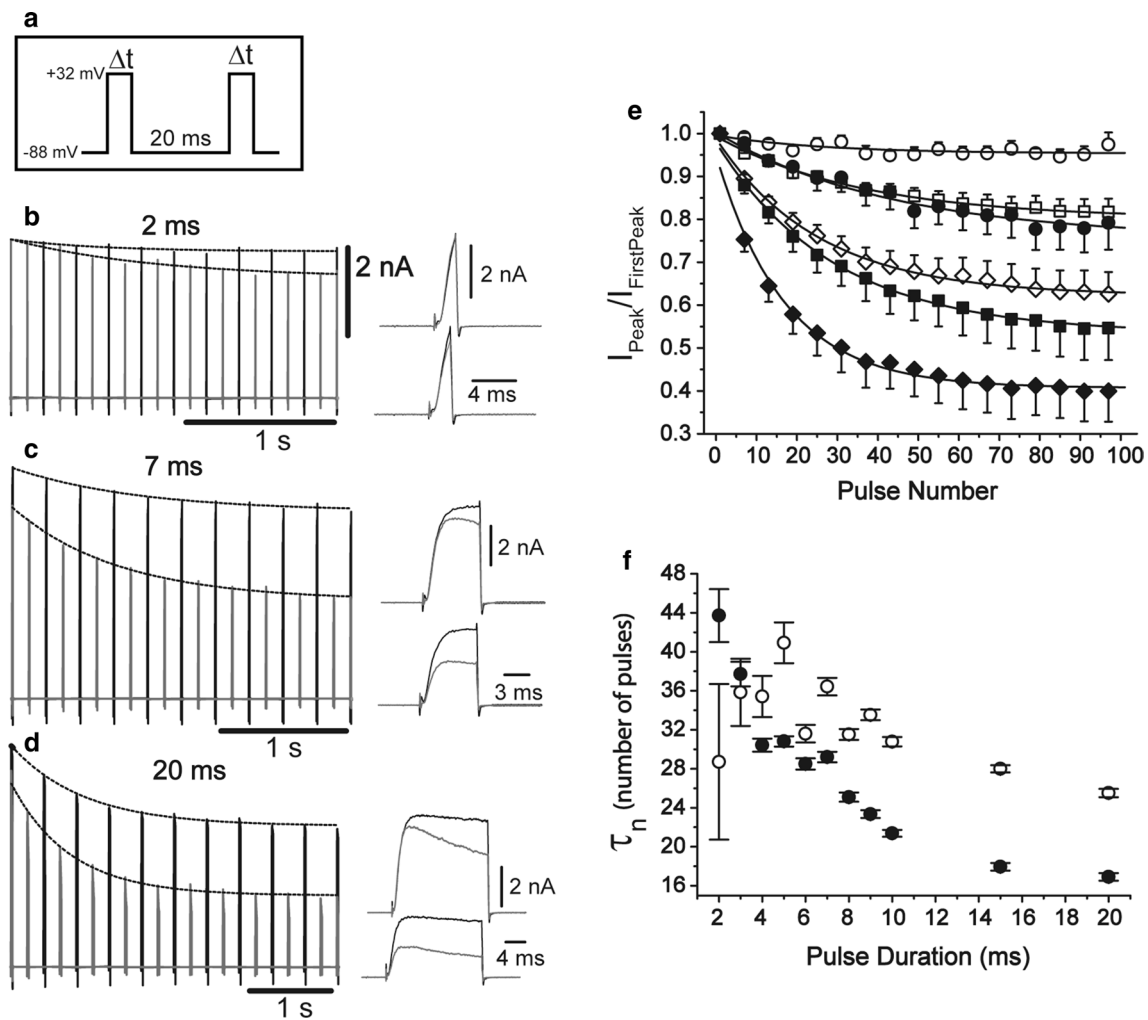


**Fig. 8** Longer depolarizations enhance SMD2 blockade. **a** Voltage protocol depolarizing pulses from  $-88$  to  $+32$  mV, with varying durations ( $\Delta t = 2, 3, 4, 5, 6, 7, 8, 9, 10, 15$  and  $20$  ms), and a fixed pulse interval of  $20$  ms were applied 101 times. **b–d** are representative current responses for pulse duration of  $2, 7$  and  $20$  ms, respectively. On the right side of **b–d** are representative traces for the first (upper traces) and last pulse (lower traces) in an expanded time scale. Black lines indicate the control situation and gray lines in the presence of SMD2. **e** Ratios of a given peak in relation to the first peak of the current for control (open symbols) and in the presence

of SMD2 (closed symbols), versus pulse number (pulses duration are open circles, filled circles =  $2$  ms; open square, filled square =  $7$  ms and open diagonal, filled diagonal =  $20$  ms). For clarity purposes only one every 6-point obtained from the total number of pulses, was plotted. Solid lines are best fits of a single exponential function to the data points. **f** Is a plot of the time constants, expressed as number of pulses, calculated from data shown in **e** against their respective pulse durations ( $N = 7$ ). Note we are expressing the time constants in terms of pulse numbers, instead of time, because the effects are more clearly appreciated

of SMD2 (closed symbols), versus pulse number (pulses duration are open circles, filled circles =  $2$  ms; open square, filled square =  $7$  ms and open diagonal, filled diagonal =  $20$  ms). For clarity purposes only one every 6-point obtained from the total number of pulses, was plotted. Solid lines are best fits of a single exponential function to the data points. **f** Is a plot of the time constants, expressed as number of pulses, calculated from data shown in **e** against their respective pulse durations ( $N = 7$ ). Note we are expressing the time constants in terms of pulse numbers, instead of time, because the effects are more clearly appreciated

of TEA on potassium currents of the squid giant axon. This argument is supported by several results shown here.

Figure 2b also shows that fitting the Hill equation to the data points results in  $N = 1.9$  for current and  $1.7$  for charge transferred, suggesting that at least two molecules of SMD2 are necessary to block the channel. This is like results reported by Brock for *S*-nitrosodithiothreitol on Shaker potassium channel ( $n = 2$ ) (Brock et al. 2001), for sibutramine on K<sub>v</sub>3.1 ( $n = 1.6$ ) (Kim et al. 2007), and fluoxetine on K<sub>v</sub>3.1 ( $n = 1.4$ ) (Sung et al. 2008). The  $IC_{50}$  resulting from the Hill equation is equal to  $9.3 \mu\text{M}$ , evaluated from the current, and  $13.5 \mu\text{M}$  for the total charge transferred.

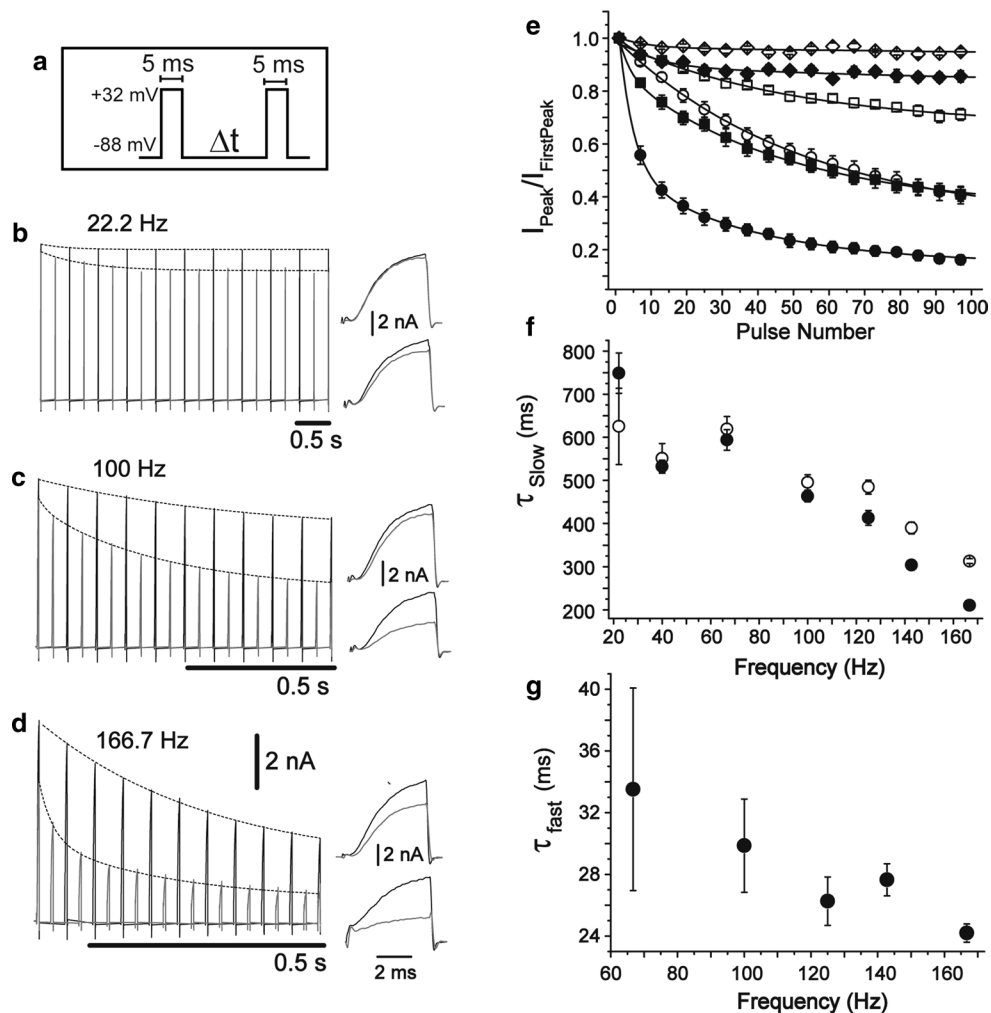


**Fig. 9** Use dependent effect of SMD2. **a** Voltage protocol: 101 depolarizing voltage pulses were applied from  $-88$  to  $+32$  mV with duration of 5 ms. The interpulse interval was varied to obtain different frequencies of stimulation (10, 12.5, 22.2, 40, 100, 125, 142, and 166.7 Hz). **b–d** Show representative traces for stimulation frequencies of 22.2, 100 and 166.7 Hz, respectively. The traces on the right of **b–d** are the individual pulses (first–upper) and (last–lower) on an expanded time scale. Traces in black refer to the control situation and in gray in the presence of  $13.5 \mu\text{M}$  SMD2. **e** Shows the normalized peak currents in relation to the first peak ( $I_{\text{Peak}}/I_{\text{FirstPeak}}$ ) plotted

against the time taken to apply the 101 pulses at the given frequency. Open symbols refer to the control situation and filled symbols in the presence of SMD2 (open diagonals, filled diagonals = 22 Hz; open squares, filled squares = 100 Hz; open circles, filled circles = 166.7 Hz). For clarity purposes only one every 6 points, from the train of pulses, was plotted. Solid lines are best fits of a single exponential (22 Hz) or double exponential (100 and 166.7 Hz) function to the data points. **f**, **g** Are plots of the slow and fast time constants, respectively, against frequency (for each frequency of stimulation), obtained from plots like the ones in **e** ( $N = 8$ )

These values are similar to the reported for other blockers of  $K_{\text{v}}3.1$ , such as fluoxetine ( $13.4 \mu\text{M}$ ) (Sung et al. 2008), smaller than sibutramine ( $32.7 \mu\text{M}$ ) (Kim et al. 2007) and TEA ( $200 \mu\text{M}$ ) (Grissmer et al. 1994), and larger than norfluoxetine ( $0.80 \mu\text{M}$ ) (Choi et al. 2001) and gambierol ( $1.2 \text{ nM}$ ) (Kopljar et al. 2009).

Since SMD2 is negatively charged under the conditions of our experiments, it is expected that voltage might affect its blocking effectiveness. In fact, blocking is maximal around  $+30$  mV and it starts to decrease for strongly depolarized voltages, suggesting a possible block relief. This can also be seen in Fig. 3b, where the voltage dependence of the

normalized conductance is described by the sum of two Boltzmann functions: the first with a steeper slope, and shifted to the left in relation to control, and the second displaying shallower voltage dependence. Blocking relief is a phenomenon reported to occur in other channels and for other drugs (Heginbotham and Kutluay 2004). The mechanism is normally associated to an effect on the inactivation. For instance, external potassium decreases C-type inactivation in  $K_{\text{v}}1$  channels, which are rapidly inactivating (Baukowitz and Yellen 1996). In our experiments, this does not seem to be the case, since increasing external  $\text{K}^+$  leads to an enhancement of inactivation in control condition and a

stronger effect of SMD2 (data not shown). In fact, for 75 and 155 mM of external potassium, the blocking relief is almost nonexistent. A similar effect was observed by Ikeda and Korn (1995) for the block of TEA on K<sub>v</sub>2.1. We also note that inactivation is accentuated when the external potassium concentration is high. This is in agreement with the suggestion that the K<sub>v</sub>3.1 has a U-type inactivation mechanism (Klemic et al. 2001).

Binding of SMD2 to the channel speeds up the rate of rise of the current upon application of a depolarizing pulse, i.e.,  $\tau_{\text{activation}}$  is significantly larger in the presence of the drug (Fig. 5a). On the other side, the deactivation process is accelerated and SMD2 has only a minor effect on the voltage dependence of the process (Fig. 5b, c). This is consequence of the fact that the channel needs to unblock before it returns to the closed state, dwelling in the open state for a longer time. This phenomenon is responsible for the crossover observed in the tail currents (inset to Fig. 5b). Nevertheless, as noted earlier, the decay of the current observed here is due to both inactivation and block of the channels (Fig. 6c). Therefore, the question that remains is: does K<sub>v</sub>3.1 inactivate when SMD2 is bound to its site or the channel must be unblocked (open) before inactivation occurs? This question can be answered by noting that SMD2 slows the time for recovery of inactivation as shown in Fig. 7, although the structural and molecular basis of U-type inactivation is not fully understood (Cheng et al. 2011; Jamieson and Jones 2013). In other words, the channel requires a longer hyperpolarized holding voltage to be fully activated in the presence of SMD2. This indicates that the channel must first be unblocked to inactivate. Additionally, SMD2 induces a shift to the right in the relationship between fraction of inactivation and voltage (Fig. 6b), indicating that in presence of SMD2 the channel leaves the blocked state to the open state, instead of going from the inactivated state to the open state.

Recently, Boddum et al. (2017) described the action of two molecules (Ex15 and RE01) that enhanced K<sup>+</sup> currents carried by K<sub>v</sub>3.1, both in *Xenopus* oocytes and in rat hippocampal slices. Contrary to our results they show an enhancement in firing frequency of AP, provoking both faster repolarization and shorter durations of action potentials. Although we have not measured AP from neurons that are expressing K<sub>v</sub>3.1, we believe that SMD2 will act in an opposite way, promoting a slower repolarization, a longer duration of AP, and an increased refractory period.

## Conclusion

Taken together, our results show that SMD2 acts mainly as an open channel blocker of K<sub>v</sub>3.1 in time-, voltage- and state-dependent manner. From a pharmacological point of view, SMD2 can be viewed as a modulator of the activity

of channels present in cells which fire at high frequencies. Besides this, our data show that a molecule supposed to act mainly as antibacterial may also serve as an ion channel blocking agent of K<sub>v</sub>3.1 channels.

**Acknowledgements** We are thankful to MSc Carina Couto Martins for synthesis of benzenesulfonamide, to Dr. André Dagostin and Fernando Aguiar for technical assistance; Dr. Dario Zamboni for providing us the wild type L929 cells and Dr. Ricardo Mauricio Leão and Davi Moraes for lab facilities. This work was supported by Coordenação de Aperfeiçoamento de Pessoal de Nível Superior-CAPES (PhD fellowship-Carlos Alberto Zanutto Bassetto Jr.) and Fundação de Amparo à Pesquisa do Estado de São Paulo-FAPESP for research funding of Professors Wamberto Antonio Varanda (2012/19750-7) and Eduardo René Pérez. González (2013/24487-6), respectively.

## Compliance with ethical standards

**Conflict of interest** The authors declare that they have no conflicts of interest.

**Research involving human participants and/or animals** This article does not contain any studies with human participants or animals performed by any of the authors.

**Informed consent** This article does not contain any studies with human participants performed by any of the authors.

## References

- Aiyar J, Nguyen AN, Chandy KG, Grissmer S (1994) The P-region and S6 of Kv3.1 contribute to the formation of the ion conduction pathway. *Biophys J* 67:2261–2264
- Armstrong CM (1969) Inactivation of the potassium conductance and related phenomena caused by quaternary ammonium ion injection in squid axons. *J Gen Physiol* 54:553–575
- Baukrowitz T, Yellen G (1996) Use-dependent blockers and exit rate of the last ion from the multi-ion pore of a K<sup>+</sup> channel. *Science* 271:653–656
- Boddum K, Hougaard C, Xiao-Ying Lin J, von Schoubye NL, Jensen HS, Grunnet M, Jespersen T (2017) Kv3.1/Kv3.2 channel positive modulators enable faster activating kinetics and increase firing frequency in fast-spiking GABAergic interneurons. *Neuropharmacology* 118:102–112
- Brock MW, Mathes C, Gilly WF (2001) Selective open-channel block of Shaker (Kv1) potassium channels by *s*-nitrosodithiothreitol (SNDTT). *J Gen Physiol* 118:113–134
- Cheng YM, Azer J, Niven CM, Mafi P, Allard CR, Qi J, Thouta S, Claydon TW (2011) Molecular determinants of U-type inactivation in Kv2.1 channels. *Biophys J* 101:651–661
- Choi BH, Choi J-S, Yoon SH, Rhie D-J, Min DS, Jo Y-H, Kim M-S, Hahn SJ (2001) Effects of norfluoxetine, the major metabolite of fluoxetine, on the cloned neuronal potassium channel Kv3.1. *Neuropharmacology* 41:443–453
- Gan L, Kaczmarek LK (1998) When, where, and how much? Expression of the Kv3.1 potassium channel in high-frequency firing neurons. *J Neurobiol* 37:69–79
- Grissmer S, Ghanshani S, Dethlefs B, McPherson JD, Wasmuth JJ, Gutman GA, Cahalan MD, Chandy KG (1992) The Shaw-related potassium channel gene, Kv3.1, on human chromosome-11,

- encodes the type-L K<sup>+</sup> channel in T-cells. *J Biol Chem* 267:20971–20979
- Grissmer S, Nguyen AN, Aiyar J, Hanson DC, Mather RJ, Gutman GA, Karmilowicz MJ, Auperin DD, Chandy KG (1994) Pharmacological characterization of five cloned voltage-gated K<sup>+</sup> channels, types Kv1.1, 1.2, 1.3, 1.5, and 3.1, stably expressed in mammalian cell lines. *Mol Pharmacol* 45:1227–1234
- Gross MF, Beaudoin S, McNaughton-Smith G, Amato GS, Castle NA, Huang C, Zou A, Yu W (2007) Aryl sulfonamido indane inhibitors of the Kv1.5 ion channel. *Bioorg Med Chem Lett* 17:2849–2853
- Gross MF, Castle NA, Zou A, Wickenden AD, Yu W, Spear KL (2009) Aryl sulfonamido tetralin inhibitors of the Kv1.5 ion channel. *Bioorg Med Chem Lett* 19:3063–3066
- Hamill OP, Marty A, Neher E, Sakmann B, Sigworth FJ (1981) Improved patch-clamp techniques for high resolution current recording from cells and cell-free membrane patches. *Pflügers Arch* 391:85–100
- Heginbotham L, Kutluay E (2004) Revisiting voltage-dependent relief of block in ion channels: a mechanism independent of punch-through. *Biophys J* 86:3663–3670
- Hille B (2001) Potassium channels and chloride channels. In: Hille B (ed) *Ion channels of excitable membranes*. Sinauer Associates Inc, Sunderland, pp 131–167
- Ikeda SR, Korn SJ (1995) Influence of permeating ions on potassium channel block by external tetraethylammonium. *J Physiol* 486:267–272
- Jamieson Q, Jones SW (2013) Role of outer-pore residue Y380 in U-type inactivation of Kv2.1 channels. *J Membr Biol* 246:633–645
- Kim SE, Ahn HS, Choi BH, Jang H-J, Kim M-J, Rhie D-J, Yoon S-H, Jo Y-H, Kim M-S, Sung K-W, Hahn SJ (2007) Open channel block of A-type, Kv4.3, and delayed rectifier K<sup>+</sup> channels, Kv1.3 and Kv3.1, by sibutramine. *J Pharmacol Exp Ther* 321:753–762
- Klemic KG, Kirsch GE, Jones SW (2001) U-type inactivation of Kv3.1 and Shaker potassium channels. *Biophys J* 81:814–826
- Kopljar I, Labro AJ, Cuyper E, Johnson HWB, Rainier JD, Tytgat J, Snyders DJ (2009) A polyether biotoxin binding site on the lipid-exposed face of the pore domain of Kv channels revealed by the marine toxin gambierol. *Proc Natl Acad Sci USA* 106:9896–9901
- Li W, Kaczmarek LK, Perney TM (2001) Localization of two high-threshold potassium channel subunits in the rat central auditory system. *J Comp Neurol* 437:196–218
- Lien C-C, Jonas P (2003) Kv3 potassium conductance is necessary and kinetically optimized for high-frequency action potential generation in hippocampal interneurons. *J Neurosci* 23:2058–2068
- Lloyd J, Atwal KS, Finlay HJ, Nyman M, Huynh T, Bhandaru R, Kover A, Schmidt J, Vaccaro W, Conder ML, Jenkins-West T, Levesque P (2007) Benzopyran sulfonamides as Kv1.5 potassium channel blockers. *Bioorg Med Chem Lett* 17:3271–3275
- Martins CC, Bassetto CAZ, Santos JM, Eberlin MN, Magalhães A, Varanda WA, Gonzalez ERP (2016) Mass spectrometry study of *N*-alkylbenzenesulfonamides with potential antagonist activity to potassium channels. *Amino Acids* 48:445–459
- McCrossan ZA, Lewis A, Panaghie G, Jordan PN, Christini DJ, Lerner DJ, Abbott GW (2003) MinK-related peptide 2 modulates Kv2.1 and Kv3.1 potassium channels in mammalian brain. *J Neurosci* 23:8077–8091
- Olsson RI, Jacobson I, Iliefski T, Boström J, Davidsson Ö, Fjellström O, Björe A, Olsson C, Sundell J, Gran U, Gyll J, Malmberg J, Hidestål O, Emtenäs H, Svensson T, Yuan Z-Q, Strandlund G, Åstrand A, Lindhardt E, Linhardt G, Forsström E, Höglberg Å, Persson F, Andersson B, Rönborg A, Löfberg B (2014) Lactam sulfonamides as potent inhibitors of the Kv1.5 potassium ion channel. *Bioorg Med Chem Lett* 24:1269–1273
- Ousingsawat J, Spitzner M, Puntheeranurak S, Terracciano L, Tornillo L, Bubendorf L, Kunzelmann K, Schreiber R (2007) Expression of voltage-gated potassium channels in human and mouse colonic carcinoma. *Clin Cancer Res* 13:824–831
- Rodrigues ARA, Arantes EC, Monje F, Stühmer W, Varanda WA (2003) Tityustoxin-K(α) blockade of the voltage-gated potassium channel Kv1.3. *Br J Pharmacol* 139:1180–1186
- Rudy B, McBain CJ (2001) Kv3 channels: voltage-gated K<sup>+</sup> channels designed for high frequency repetitive firing. *Trends Neurosci* 24:517–526
- Shieh C-C, Coghlan M, Sullivan JP, Gopalakrishnan M (2000) Potassium channels: molecular defects, diseases, and therapeutic opportunities. *Pharmacol Rev* 52:557–593
- Sung MJ, Ahn HS, Hahn SJ, Choi BH (2008) Open channel block of Kv3.1 currents by fluoxetine. *J Pharmacol Sci* 106:38–45
- Supuran CT, Scozzafava A, Jurca BC, Ilies MA (1998) Carbonic anhydrase inhibitors—part 49: synthesis of substituted ureido and thioureido derivatives of aromatic/heterocyclic sulfonamides with increased affinities for isozyme I. *Eur J Med Chem* 33:83–93
- Taskin B, von Schoubye NL, Sheykhzade M, Bastlund JF, Grunnet M, Jespersen T (2015) Biophysical characterization of Kv3.1 potassium channel activating compounds. *Eur J Pharmacol* 758:164–170
- Wang L-Y, Gan L, Forsythe ID, Kaczmarek LK (1998) Contribution of the Kv3.1 potassium channel to high-frequency firing in mouse auditory neurones. *J Physiol* 509:183–194
- Yasuda T, Cuny H, Adams DJ (2013) Kv3.1 channels stimulate adult neural precursor cell proliferation and neuronal differentiation. *J Physiol* 591:2579–2591